Desalination and Water Treatment
www.deswater.com
20 (2010) 264–271
August
1944-3994 / 1944-3986 © 2010 Desalination Publications. All rights reserved.
doi: 10.5004/dwt.2010.1602

Modeling and membrane resistance analysis of stainless steel membrane in alkali wastewater recovery processing

Liming Zhao[a], Wenshui Xia[a]*, Hefei Zhao[a], Zhiwei Xu[b], Xiaoyan Wu[b], Jun Zhao[b]

[a]*State Key Laboratory of Food Science and Technology, School of Food Science and Technology, Jiangnan University, 1800, Lihu Avenue,Wuxi City, Jiangsu Province 214122, China*

Tel. +86 (510) 85919121; Fax +86 (510) 85329057; email: xiaws@jiangnan.edu.cn

[b]*Hydrochem Engineering (Shanghai) Co., Ltd. 99 JuLi Road, Zhangjiang Hi-Tech Park, Pudong Area, Shanghai 201203, China*

Received 8 October 2009; Accepted in revised form 26 January 2010

ABSTRACT

A semi-empirical cross-flow ultrafiltration (UF) model of stainless steel membrane that can predict permeate flux as a function of treatment time with alkali wastewater in chitin production was studied. A tubular stainless steel membrane supplied by Hyflux® (Singapore) was employed. Alkali wastewater from chitin deproteination process with 3.4% NaOH (W/W) and 1.7% protein and its hydrolysate was used as the feed liquid. The permeate flux of the pure water was performed under different conditions and the membrane resistance was obtained, and the growth models were developed and analyzed. The resistance that leads to the flux decline was measured, and the model predictions were compared with the experimental data obtained from pilot plant operation. Results showed that the growth model could used to predict the flux decline of SSM very well, and the correlation coefficient was determined as 0.9892.

Keywords: Stainless steel membrane; Flux decline; Growth curve model; Membrane fouling; Membrane resistance

1. Introduction

In chitin industry, the high sodium hydroxide consumption leads to high production costs and severe environmental issues [1]. The wastewater from the alkali deproteination step contains a high concentration of NaOH, certain amount of protein, little lipids and suspended solid (SS). The COD of the wastewater is high up to 7000–8000 mg/kg, and the SS ranges from 800 to 1200 mg/kg. The recovery of NaOH by stainless steel membrane (SSM) ultrafiltration coupled with nanofiltration would make perfect sense from both ecological and economic points of view.

Crossflow ultrafiltration (UF) or microfiltration (MF) is an efficient method for clarification of some suspensions and resolvable large molecular materials. However, the performance of UF and MF in many applications is limited by membrane fouling, which causes decay in permeate flux and leads to a high capital cost of membrane equipment, high operation cost and expensive cleaning cost [2]. This phenomenon refers to the deposit of rejected particles of the feed components on the surface of the membrane, and the adsorption of small particles such as protein and macromolecules within the membranes pores [3].

Membrane fouling is due to specific physical or chemical interactions between solutes particle and membrane.

* Corresponding author.

The continuously decline of the flux was explained differently in various studies, indicating the difficulty in modeling the process [4]. The internal fouling is characterized by particles adsorption on the pores walls and mouths, and the external fouling is due to the deposition and the growth of particles aggregates on the membrane surface leading to the built-up of a cake layer. For SSM system, different types of fouling predominates the resistance of membrane during different period of processing time for various feeds. Physical fouling is the main type in the referred alkali wastewater from chitin production in this work .The fouling contributes to the total resistance of the membrane. In order to prevent the fouling phenomenon, a good understanding of the mechanism is necessary, and it can be achieved by a modeling step.

Models for flux decline can help predict permeate fluxes. Models are also very useful for industry to select the optimal operating parameters and estimate capital cost and operation cost.

Some recent empirical or semi-empirical UF/MF resistance and flux decline models have been developed [5]. Song et al. divided the total resistance into membrane resistance, adsorption resistance and cake resistance, and also set out relatively resistance models, and the flux decline model was achieved by using Darcy's law [6,7]. Zhang et al. theoretically analyzed the blocking mechanism of the MF fouling based on the blocking experiments, and improved traditional resistance models, which can better explain the blocking phenomena of MF fouling [8]. A gel polarization model was used to explain the external fouling. The gel polarization or cake filtration model considered that the cake layer provides additional resistance due to deposition of rejected particles on the membrane surface and therefore increases with time.

These established models, however, can not well predict the ultrafiltration processing of the alkali wastewater by SSM. Therefore, the objective of this work was to analyze the fouling resistance and to develop a mathematical model of SSM of cross-flow process of industrial scale alkali wastewater, based on the basic membrane separation theories and pilot experimental data. The modeling results were compared with experimental data. The results could provide directions of process optimization of unit operation of SSM, especially in the field of the recovery of caustic sodium in chitin process and similar alkali wastewater treatment system such as milk CIP wastewater treatment. The method of growth curve modeling for SSM UF membrane is a novel job that can predict flux decline of membrane very well.

2. Experimental

2.1. Materials

The alkali wastewater (AW) which contained 3.4% of NaOH(w/w), 1.7g/L(based on total nitric,6.25) of proteins and protein degradation products from the industrial chitin processing was supplied by Haipu Biological Co., Ltd. (China). HNO_3 and NaOH flakes of chemical grade were used for membrane cleaning. The main components in the wastewater are listed in Table 1.

Table 1
Main components in the wastewater used for feed solution

Chemical	Parameter
C_{NaOH}, %	3.42
Na^+, mg/L	195.80
Ca^{2+}, μg/L	148.4
COD, g/L	5.779
$C_{protein}$, g/L	1.7
SS, mg/L	1100

2.2. Membranes

Ferrosep 20 tubular stainless steel membrane (SSM) was supplied by Hyflux® (Singapore). Pilot-scale SSM contained four monochannel tubular modules with 1.5 m in length, 18.3 mm inner diameter and 21.6 mm outer diameter. The membrane pore size was 20 nm in average with the molecular weight-cut-off (MWCO) at 20,000 Da. The pilot SSM had 0.35 m^2 membrane area. This membrane was made of a porous 316L stainless steel tube surface-coated with a sintered TiO_2 layer, which can resist extreme pH (0–14) and temperature (up to 200°C), the detailed parameters of the SSM are listed in Table 2. Fig. 1 shows the structure of the module.

2.3. Pilot equipment

The pilot plant (L-400) supplied by Hydrochem (China) was employed in this work, which was especially designed for this research (Fig. 2). The plant consists of one circulation loop, meaning that the cleaning circulation shared with the feed one. The feed tank of 1 ton capacity

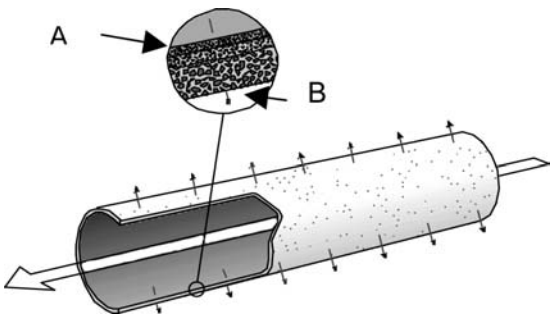

Fig. 1. The structure of the SSM tubular module. A: Sintered TiO_2 membrane layer nominally 0.02 micron; B: Porous 316L stainless steel substrate — 1.0 μm.

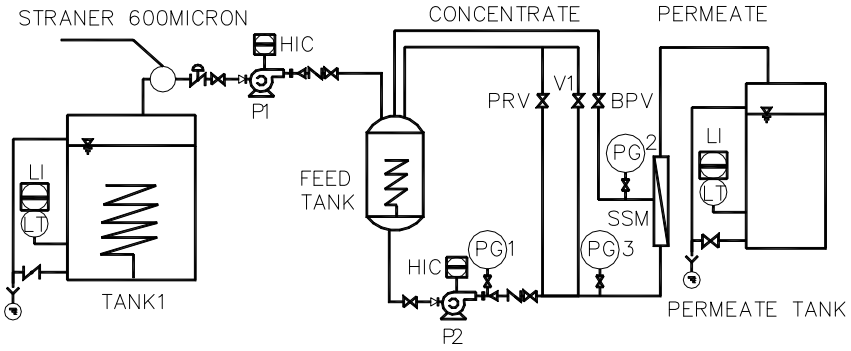

Fig. 2. Schematic diagram of pilot plant. P1, P2 — feed pump and cycle pump; PG1, PG2, PG3 — pressure gauge.

Table 2
Parameter settings used for the model simulation studies [9]

Parameter	Value
Diameter (nominal/outer/inner), mm	19.0/21.6/18.3
Wall thickness, mm	1.65
pH range	0–14
Maximum temperature, °C	up to 200
Maximum pressure, bar	up to 70
Recommended operating pressure, bar	2–6

included a mixer to homogenize the feed solution and a heat exchanger for temperature control. A 600-micron pre-filter was placed upstream of a feed pump (P1); next to the feed tank was the circulation pump (P2), and a ENSNAL—MORET chemical pump (MFR 50 32 200, France) was used to pump the feed through the equipment and provide the cycle pressure. Next to the circulation pump exists there was a manometer (PG1) measuring the pump pressure. Two manometers (PG2 and PG3) placed at both sides of the membrane module measured the pressure drop across them. The retentate was back to the feed tank, while the permeate flowed to a reservoir. Retentate valve and bypass valve situated just after the PG2 and before PG3 were used to regulate the TMP. The permeate flux was volumetric measured by a cylinder.

2.4. Filtration experiments

2.4.1. Membrane characterization experiments

Several experiments by deionized water under different TMPs (2, 2.5, 3, 3.5 and 4 bar) at 70°C were performed to determine the water permeability and membrane resistance. In all experiments the cross-flow velocity was fixed at 4 m/s. The temperature was controlled by heat exchanger.

2.4.2. Fouling experiments

The AW used as feed in this work was heated by heat exchanger to 65–70°C, and then it was pumped into the feed tank. The pilot plant was stopped after 8 h of operation, when the flux was stable and the fouling was reach quasi-steady-state.

The operation TMP was set to 2.3 bar and the flow rate was set to 4 m/s. During the operation the temperature varied between 65°C to 75°C due to the circulation heating. All the experiments were employed the same membrane and pilot plant. The membrane was cleaned after each runs, and the water permeate flux before and after cleaning were measured.

2.4.3. Membrane cleaning

The membrane was cleaned after each experiment according to the following steps:

- Rinsing with tap water for 5 min;
- Cleaning with HNO_3 solution of 2% in deionized water for 20 min;
- Rinsing with deionized water to neutral;
- Cleaning with 2% of NaOH in deionized water and 500 ppm of EDTA-Na for 20 min;
- Rinsing with deionized water to neutral.

Every cleaning step by acid or caustic soda was performed at 60°C, and a TMP of 0 bar and a cross-flow velocity of 4 m/s was set. The membrane flux for deionized water was measured before and after each run, and the after cleaning water flux should be equal or close to that of before experiment.

2.4.4. Data processing

Data processing and mathematic modeling was carried out using Matlab™ R2007a scientific computer program, including "polyfit" command for simulating linear equation, and "lsqcurvefit" command for simulating non-linear equation, and "ode45" command for

differential equation resolving, and "corrcoef" command for calculating correlation coefficient matrix between experimental data and model simulation.

3. Theory

3.1. Mechanism of SSM ultrafiltration fouling

The process of ultrafiltration separation was divided into several stages as follows: Initial filtration stage, during which mass of the small particles permeate into the clean pore of the membrane, and among of them some of particles were adsorbed into the pore due to various forces. And the pore adsorption decreases the efficient pore diameter. During this stage the internal fouling dominates [10,11], while the large particles were retentated on the surface of the membrane, and the loose porous cake layer began to form.

The large particles were taken away on the external surface replaced by the small particles, when the pore adsorption started to saturate. The loose porous cake layer formed by large particles during initial stage was gradually pressed out, and the external fouling of membrane becomes to predominate.

As the thickness of the cake layer increased gradually, the percentage of small particles within the cake increased too. Smaller particles permeated into the formed cake layer led to that the small particles could not reach the pore, and ultimately the gel cake layer was formed on the surface of the membrane. In this stage, the permeate flux becomes stable [12]. Fig. 3 shows the pore blocking, pore adsorption and cake layer forming course.

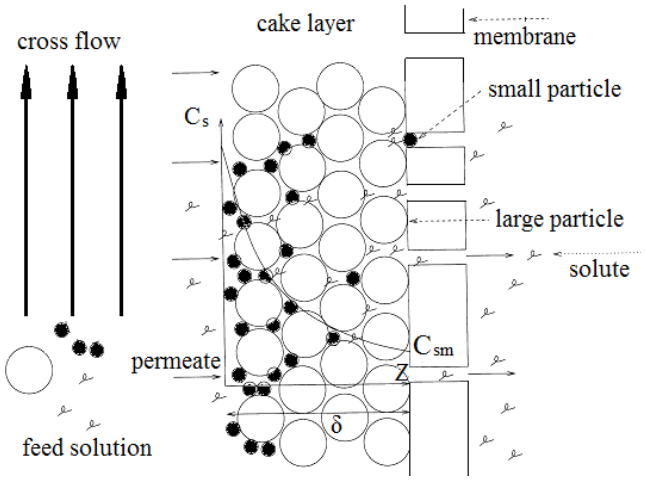

Fig. 3. Schematic of a cake layer and pore adsorption and deposition of large and small particles, the cake layer is the secondary membrane. C_s — concentration of small particle on the cake layer surface; C_{sm} — concentration of small particle on the membrane surface; Z — axis of permeation; δ — thickness of cake layer.

3.2. Analysis of fouling resistances

The flux at any location in the membrane filtration channel is governed by the so-called general filtration equation given as [6]:

$$J = \frac{dV}{Adt} = \frac{\Delta P}{\mu_s R_t} \quad (1)$$

$$R_t = R_m + R_a + R_c \quad (2)$$

where J is the permeate flux (LMH, $Lm^{-2}h^{-1}$), ΔP is the applied transmembrane pressure (TMP, bar), V is the permeate volume (L), A is the efficient membrane area (m^2), t is the filtration time (h), μs is the viscosity of feed (mPa.s), and R_t, R_m, R_a and R_c are the total resistance, membrane resistance, adsorption resistance and resistance of the concentration polarization layer and the resistance of the cake layer, respectively (m^{-1}).

R_t is the total resistance during the filtration, including the membrane hydraulic resistance (R_m), and the resistance due to membrane fouling and concentration polarization (R_f). R_f can be further divided into R_a and R_c. R_a is an adsorption resistance because of the physical or chemical interaction between particles and membrane pore inner wall and entrance and membrane surface, and it increases rapidly in the initial filtration stage and plays an important role on the flux decline. R_c is the cake layer resistance produced by particle deposition layer formation, and sometimes it includes the effect of concentration polarization (CP). R_c plays a dominant role in the flux decline in respect to filtration time in the middle and later stage of the filtration. The CP phenomenon exists in all kinds of membrane filtration processes, and the CP layer will add an additional resistance which we hereby considered together with the cake layer resistance. However, the effect of CP resistance can be reduced by modifying the applied pressure to increase the membrane surface flow velocity.

R_a and R_c vary with the filtration time, and their values are directly related to the permeate flux. As to various of feeds and membranes, the reasons that produce the R_a and R_c are different, and the roles they plays during different filtration stages are also different.

Dal-Cin et al. pointed out that it would be estimated much higher for the CP resistance while much lower for the resistance due to the particle adsorption, when comparing to the relative ratio between all parts of resistances by modeling the above mentioned resistances [13]. The distribution of the fouling resistances between the adsorption resistance and cake layer resistance usually depends on the accuracy of the adopted model, and their practical application is more complex. Hence, the definition of membrane fouling resistance in this report is defined to cover the R_c and R_a to develop a simple and easy to use model. The fouling resistance is defined as:

$$R_f = R_a + R_c \tag{3}$$

So the total resistance can be simplified as:

$$R_t = R_m + R_f \tag{4}$$

4. Model description

Growth curve models [14,15] can descript the complete course including occurring, developing and maturing of things. It is an important method of trend extrapolation, which is already widely applied to elucidate biology mass growth (for example, the growth curve of microbial, reproduction of cells and the growth of human population), some technologies and economic fields. The growth of biomass such as the growth of human population and reproduction of cells increase following the law of exponential function, when it reaches a certain biology density level, it gradually goes to a steady state or a limitation due to the restriction of environmental and itself.

Famous models include Logic model, Pearl model, Ridenour model and Gompertz model, and there are a lot of specific equations of those models. The main pattern is S-curve, which reflects the development principle of a thing restricted by a pair of illogicality [16]. Generally, growth models have the characteristic that the initial increase changes rapidly and later tends to smooth and steady, which is similar with the increase trend of membrane fouling resistance. The common rule of the Pearl model, Ridenour model and Gompertz model is the relative diversification ratio of the characteristic parameter R_f/k is a function of its relative level, namely the general equation of growth S-curve can be expressed as:

$$\frac{1}{R_f}\cdot\frac{dR_f}{dt} = f\left(\frac{R_f}{k}\right) \tag{5}$$

where k is the fouling resistance control parameter and $f(R_f/k)$ is a random function of R_f/k, it is called a relative level function of the characteristic parameter.

A new growth curve model can be developed by properly selecting the function $f(R_f/k)$, in order to descript more variation trends. Generally, Eq. (6) is recommended:

$$f\left(\frac{R_f}{k}\right) = a\cdot\left(1-\frac{R_f^n}{k^n}\right) \tag{6}$$

where a is the time control parameter. Here n is usually selected as a certain value, for instant, $n = 0.5$, $n = 1$, $n = 2$, but it was found in this study that n controls the S-curve growth to reach steady-state, so n can be defined as the characteristic parameter of the model in order to obtain the more universal growth model. Combining Eq. (5) and (6) and integrating, Eq. (7) was obtained:

$$R_f = \frac{k}{\sqrt[n]{1+\left(\frac{k^n}{{R_{f0}}^n}-1\right)\cdot e^{-2a\cdot(t-t_0)}}} \tag{7}$$

where R_{f0} is the initial membrane fouling resistance and t_0 is the initial filtration time. In general, the theory value of the R_{f0} is 0, because the initial filtration time is 0, as to the membrane fouling resistance. However, in experiments the flux of 0 time was difficult to be measured, the tested initial fouling value was not 0. Calculated from Eq. (4), the R_{fo} is 0.1338×10^9 m^{-1}.

In this modeling, it was assumed that the composition of the fed alkali wastewater was kept constant or varied little among different batches, so that the effect of the concentration of the feed could be ignored.

Combined Eqs. (1),(4) and (7), and integrating of the value of μ_s yields:

$$J = \frac{dV}{A\cdot dt} = \frac{\Delta P}{\mu_s\cdot R_t} = \frac{\Delta P}{\mu_s\cdot\left(R_m+R_f\right)} = \frac{\Delta P}{\mu_s\cdot\left[R_m+\frac{k}{\sqrt[n]{1+\left(\frac{k^n}{R_{f_0}^n}-1\right)\cdot e^{-2a(t-t_0)}}}\right]} \tag{8}$$

Eq. (8) can be expressed as Eq.(9), because the Q is the common used parameter in industry:

$$Q = \frac{dV}{dt} = \frac{\Delta P\cdot A}{\mu_s\cdot\left[R_m+\frac{k}{\sqrt[n]{1+\left(\frac{k^n}{R_{f_0}^n}-1\right)\cdot e^{-2a(t-t_0)}}}\right]} \tag{9}$$

where Q is the fluid rate of the permeate (L/h). In Eqs. (8) and (9), only k, a and n are uncertain. Both equations can descript the permeate flux or fluid rate decline in respect to filtration time.

5. Results and discussion

5.1. Membrane characterization

Pure water permeate flux was used to evaluate the membrane hydraulic resistance (R_m) according to Darcy's law [Eq. (10)] [17].

$$J_w = \frac{dV}{Adt} = \frac{\Delta P}{\mu_w R_m} \tag{10}$$

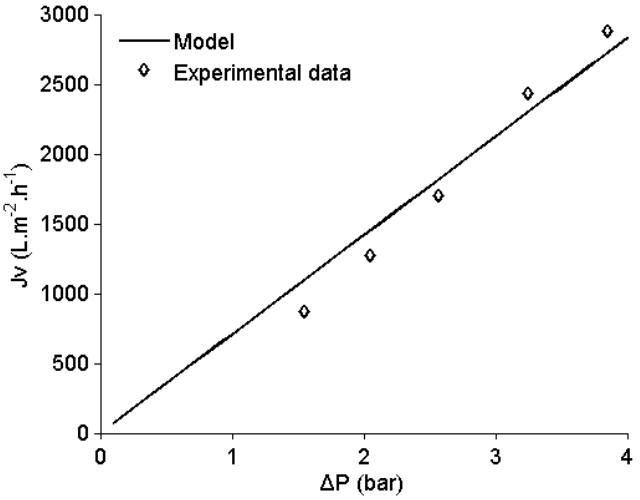

Fig. 4. Pure water permeate flux vs. TMP at 70°C.

where J_w is the pure water permeate flux (LMH) and μ_w is the hydraulic viscosity of pure water at specific temperature (mPa·s).

Fig. 4 shows the pure water permeate flux experimental data and flux model, which indicates that the pure water permeate flux linearly increased with the increase of TMP. The operation temperature 70°C was considered to coincide with the fouling experimental condition. Taking into account that the dynamical viscosity value of pure water at 70°C is 0.4061 mPa·s, the value of the membrane resistance (R_m) obtained was 1.2528×10^9 m^{-1}. Comparing the model value with the experimental data, a correlation coefficient of 0.9980 was obtained.

5.2. Simulation of the model

For real alkali wastewater solution, the multicomponent system was very complex, so it is impractical to analyze the effect of each component on the fouling resistance and permeate flux decline. The growth curve model is more suitable for predicting the fouling resistance and flux decline trends of this complex system.

The parameters k, a and n were calculated by nonlinear regression from experimental values of permeate flux vs. filtration time, using Eq. (9) according to MatlabTM R2007a scientific computer program. Table 3 shows the results.

Table 3 shows that the modeling simulation correlation coefficient values are the highest when n was undetermined and $n = 2$. Both simulation results are quite similar under both situations. Fig. 5 shows that the models both at $n = 0.1$ and $n = 1$ were not saturated, which can explain the higher values of resistance controls parameter a in Table 3. Although the results of the simulation at $n = 2$ and n = undetermined were similar, it is more universally applied when taking n as undetermined.

In the differential Eq. (8), the parameters at the right side of the equation are all constant or available values, combining with the parameter values of $k = 3.1294\times10^9$, $a = 0.6230$ h^{-1}, $R_m = 1.2528\times10^9$ m^{-1}, $\mu_s = 1.9$ mPa·s, and $R_{f0} = 0.1338\times10^9$ m^{-1}, obtained the model data at the specific condition for the specific feed. Fig. 6 compares experimental and the model curves.

Fig. 6 shows the modeling data and the model predicts the same flux decline trend as the experimental data. The correlation coefficient is 0.9892. This result

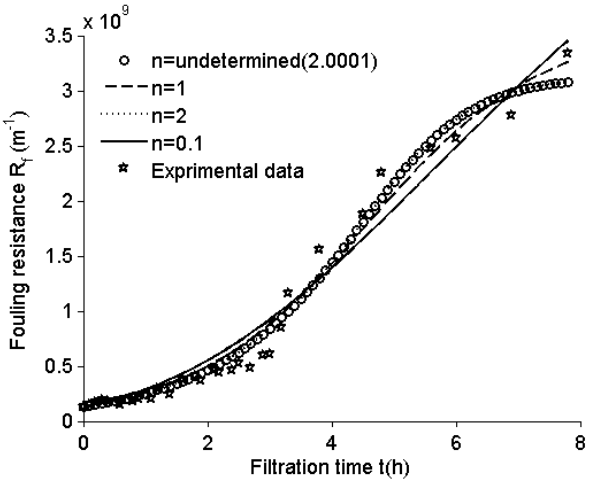

Fig. 5. Membrane fouling resistance vs. filtration time, n = 0.1, 1, 2, undetermined (2.0001). Fouling resistance models compared to experimental data. The curves were coincident at $n = 2$ and n = undetermined.

Table 3
Simulation results of fouling empirical parameter n

	$n = 1$	$n = 2$	$n = 0.1$	n = undetermined
k (10^9)	3.5871	3.1294	5.9600	3.1294
a (h^{-1})	0.7099	0.6229	0.1350	0.6230
Correlation coefficient	0.9897	0.9909	0.9836	0.9909

"n = undetermined" means that n was an undetermined parameter and computed by Matlab™ R2007a program, and the calculated result was $n = 2.0001$

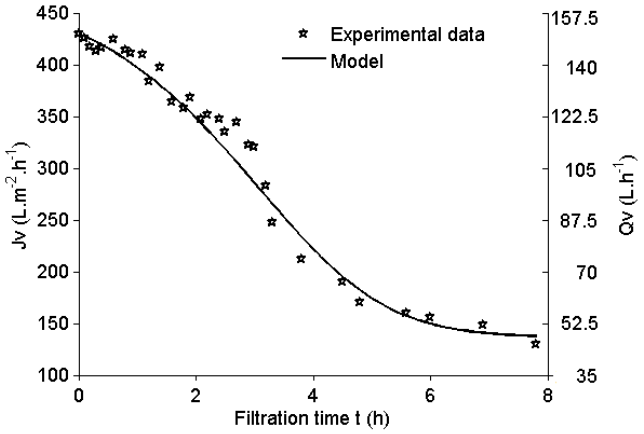

Fig. 6. The permeate flux and Q_v vs. filtration time, growth modeling data and experimental data, T = 70°C, TMP = 2.3 bar.

indicates that the established model can well predict the membrane permeate flux decline of ultrafiltration of the alkali wastewater by SSM. In industry application, the Q is the common parameter to be considered, according to Eq. (9), the volume flux decline (Q_v) model data was calculated, and the modeling data matched well with the experimental data.

6. Conclusion

The combination of the adsorption resistance and cake layer resistance as fouling resistance is suitable for the explanation of the membrane fouling resistance and flux decline, and the fouling resistance model when n is a undetermined coefficient can match well with the experimental data. The flux decline growth model developed based on the fouling resistance model can well predict the permeate flux decline trend for this kind of alkali wastewater by SSM. The correlation coefficient is 0.9892. The membrane resistance calculated from the initial permeate flux is larger than that from the pure water flux because of the initial point was not the really zero time in practical operation.

In this study, the assumption was that the components and concentration of feed solution were the same or similar in every batch. But the real alkali wastewater in chitin processing industry would fluctuate in an uncertain range due to the variation of the raw material. In future studies, the effects of feed concentration should be considered and tested.

Symbols

A — Effective membrane area, m^2
a — Time control parameter
COD — Chemical oxide demand, mg/kg
J — Permeate flux, LMH (L/m^2/h)
J_w — Pure water permeate flux, LMH (L/m^2/h)
k — Fouling resistance controls parameter
n — Characteristic parameter of model
ΔP — TMP, bar
R_a — Resistance due to pore absorption, m^{-1}
R_c — Resistance due to cake formation and concentration polarization, m^{-1}
R_f — Resistance due to membrane fouling, m^{-1}
R_{f0} — Initial membrane fouling resistance, m^{-1}
R_m — Resistance due to membrane, m^{-1}
R_t — Total resistance during filtration, m^{-1}
SS — Suspended solids, mg/kg
SSM — Stainless steel membrane
t — Filtration time, h
t_0 — Initial filtration time, h
TMP — Transmembrane pressure, bar
V — Permeate volume, L
μ_s — Dynamic viscosity of the feed, mPa·s
μ_w — Dynamic viscosity of the pure water, mPa·s

Acknowledgements

This work was financially supported by the National High Technology Research & Development Program of China (863 Program) (No. 2006AA09Z444), and it was also supported by PCSIRT0627 and 111 project-B07029. We thank Hyflux (Hydrochem, Shanghai, China) for the equipment support and helpful discussion, and Haipu Bio. Co., Ltd. (Shipu, Nibo, China) for the pilot plant and raw material support.

References

[1] T.D. Jiang, Chitin, Chem. Ind. Publishing, Beijing, 2000.
[2] S. Takizawa, K. Fujita and K.H. Soo, Membrane fouling decrease by microfiltration with ozone scrubbing, Desalination, 106 (1996) 423–426.
[3] V. Chen, A.G. Fane, S. Madaeni and I.G. Wenten, Particle deposition during membrane filtration of colloids: transition between concentration polarization and cake formation, J. Membr. Sci., 125 (1997) 109–122.
[4] F. Rouvet, K. Fiaty, I.P. Laurent and J.K. Liou, Modeling and simulation of membrane fouling in batch ultrafiltration on pilot plant, Computers Chem. Eng., 22 (1998) Suppl. S901–S904.
[5] L. Ma and G.T. Qin, Mechanism and mathematical models of membrane fouling. Technol. Wat. Treat., 33 (2007) 1–4.
[6] H. Song, Ch. Fu and Y.F. Shi, Analysis on fouling resistance and calculation of flux for microfiltration. J. Chem. Eng. Chinese Univ., 13 (1999) 315–322.
[7] H. Song, Ch. Fu and Y.F. Shi, A new mathematic model of cross-flow microfiltration and ultrafiltration. J. Sichuan Univ., 32 (2000) 52–54.
[8] J.W. Zhang and G.Y. Jin, Study on blocking of porous membrane fouling in microfiltration. Chem. Eng., 34 (2006) 38–41.
[9] About FerrocepTM, http://www.hyflux-sip.com/products/ferrocep.html.
[10] E.M. Tracy and R.H. Davis, Protein fouling of track-etched polycarbonate microfiltration membranes, J. Colloid Interf. Sci., 167 (1994) 104–116.

[11] J. Mueller and R.H. Davis, Protein fouling of surface-modified polymeric microfiltration membranes, J. Membr. Sci., 116 (1996) 47–60.
[12] L.F. Song, Flux decline in crossflow microfiltration and ultrafiltration: mechanisms and modeling of membrane fouling, J. Membr. Sci., 139 (1998) 183–200.
[13] M.M. Dal-Cin, F. McLellan, C.N. Striez, C.M. Tarn, T.A. Tweddle and A. Kumar, Membrane performance with a pulp mill effluent: relative contributions of fouling mechanisms, J. Membr. Sci., 120 (1996) 273–285.
[14] C.R. Rao. The theory of least squares when the parameters are stochastic and its application to the analysis of growth curves. Biometrika, 52 (1965) 447–458.
[15] J.E. Grizzle and D.M. Allen, Analysis of growth and dose response curves. Biometrics, 25 (1969) 357–381.
[16] S. Makidakis and S.C. Wheelwright, The Handbook of Forecasting: A Manager's Guide, John Wiley & Sons, New York,1982.
[17] B. Hu and K. Scott. Microfiltration of water in oil emulsions and evaluation of fouling mechanism. Chem. Eng. J., 136 (2008) 210–220.